

Published in final edited form as:

Environ Sci Technol. 2012 March 20; 46(6): 3398–3405. doi:10.1021/es204546u.

Efficient Degradation of TCE in Groundwater Using Pd and Electro-generated H₂ and O₂: A Shift in Pathway from Hydrodechlorination to Oxidation in the Presence of Ferrous Ions

Songhu Yuan^{†,‡}, Xuhui Mao[‡], and Akram N. Alshwabkeh^{‡,*}

[†]State Key Lab of Biogeology and Environmental Geology, China University of Geosciences, 388 Lumo Road, Wuhan, 430074, P. R. China

[‡]Department of Civil and Environmental Engineering, Northeastern University, 400 Snell Engineering, 360 Huntington Avenue, Boston, Massachusetts 02115, United States

Abstract

Degradation of trichloroethylene (TCE) in simulated groundwater by Pd and electro-generated H₂ and O₂ is investigated in the absence and presence of Fe(II). In the absence of Fe(II), hydrodechlorination dominates TCE degradation, with accumulation of H₂O₂ up to 17 mg/L. Under weak acidity, low concentrations of oxidizing •OH radical are detected due to decomposition of H₂O₂, slightly contributing to TCE degradation via oxidation. In the presence of Fe(II), the degradation efficiency of TCE at 396 μM improves to 94.9% within 80 min. The product distribution proves that the degradation pathway shifts from 79% hydrodechlorination in the absence of Fe(II) to 84% •OH oxidation in the presence of Fe(II). TCE degradation follows zeroth-order kinetics with rate constants increasing from 2.0 to 4.6 μM/min with increasing initial Fe(II) concentration from 0 to 27.3 mg/L at pH 4. A good correlation between TCE degradation rate constants and •OH generation rate constants confirms that •OH is the predominant reactive species for TCE oxidation. Presence of 10 mM Na₂SO₄, NaCl, NaNO₃, NaHCO₃, K₂SO₄, CaSO₄ and MgSO₄ does not significantly influence degradation, but sulfite and sulfide greatly enhance and slightly suppresses degradation, respectively. A novel Pd-based electrochemical process is proposed for groundwater remediation.

INTRODUCTION

Trichloroethylene (TCE) is a pollutant commonly found in soil and groundwater at contaminated sites in the United States. Processes proposed for remediation of TCE in groundwater include phase-transfer,¹ in situ chemical oxidation (ISCO),² reduction using zerovalent iron or other Fe-based materials,^{3,4} electrochemical methods,^{5,6} and bioremediation⁷. In recent years, there has been an increasing interest in electrochemical methods for treating groundwater contaminated with TCE and other chlorinated solvents.^{5,6,8–13} Direct oxidation or reduction of contaminants at anode or cathode requires suitable electrocatalytic electrode materials, which usually work at high overpotential

*To whom correspondence should be addressed. aalsha@coe.neu.edu. Phone: (617) 373-3994.

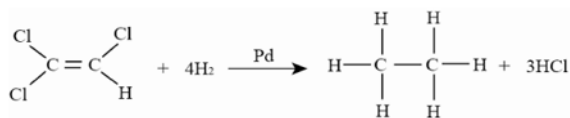
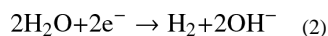
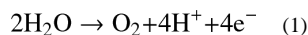
Supporting Information Available

Additional information are included for CO₂ and •OH analysis, experimental setup, control results, variation of ORP and current efficiency, pH, dissolved Fe(II) and H₂O₂ concentrations during the degradation, generation of •OH at different pH values, plots of pH and Pd/Al₂O₃ dosage versus K₀ for TCE degradation, comparison with Fenton, and a conceptual model for groundwater remediation. This material is available free of charge via the internet at <http://pubs.acs.org>.

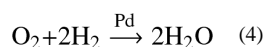
conditions to obtain vigorous redox condition for aqueous contaminants degradation. Although costly electrodes, i.e. boron doped diamond (BDD)^{5,9} and Pd-based materials¹³, can reach high degradation efficiency, it is difficult to balance between electrode cost and efficiency.

Indirect electrochemical processes provide an alternative to reduce the dependence on costly electrode materials. The function of electrodes is to sustain water electrolysis for the production of H₂ and OH⁻ at the cathode (1) along with O₂ and H⁺ at the anode (2). These products are utilized for chemical or biological degradation of contaminants. For example, O₂ produced at anode can be supplied for aerobic processes,^{12,14,15} and H₂ produced at cathode can be delivered for anaerobic degradation,^{12,15,16} or for Pd-catalytic hydrodechlorination of contaminants in groundwater.¹⁷ The OH⁻ produced at cathode could be utilized for contaminant hydrolysis.¹⁸

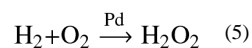
Pd can quickly hydrodechlorinate chlorinated solvents using H₂.^{19–23} Cathodic production of H₂ is also explored for Pd-catalytic hydrodechlorination of TCE in groundwater¹⁷ and the proposed transformation pathway are hydrodechlorination of TCE to ethene, followed by hydrogenation to ethane (3).^{17,19,20} Although the presence and formation of high concentrations of dissolved O₂ may suppress TCE hydrodechlorination because it is assumed to consume H₂ with production of H₂O (4); it does not appear to alter the degradation pathway.^{17,19}

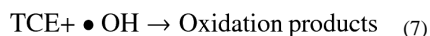
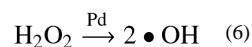


(3)

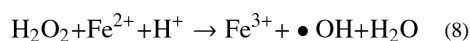


The generation of H₂O₂ from H₂ and O₂ in the presence of Pd catalyst (5)^{24,25} has never been recognized in the aforementioned investigations. H₂O₂ has the potential of oxidizing TCE in groundwater and Pd can catalyze the decomposition of H₂O₂ to a strong oxidizing •OH radical (6) (oxidation potential: 2.8 V/SHE),^{25,26} which may further oxidize TCE (7).^{5,27} Recent work highlights the efficient degradation of a recalcitrant organic pollutant by the Pd-containing electrolytic system under weak acidic conditions.²⁶ The presence of •OH was identified by electron spin resonance (ESR) assay.²⁶ However, the contribution of H₂O₂ and •OH oxidation has never been explored for TCE degradation using Pd and H₂ in the presence of O₂.





Furthermore, Fe(II) is a common species in aquifers with concentration levels on the order of mg/L.²⁸ Presence of Fe(II) is expected to impact the pathways of TCE degradation. Fe(II) can efficiently catalyze the generation of $\bullet\text{OH}$ from H_2O_2 through Fenton reaction (8).²⁹ In this case, the homogeneous oxidation by $\bullet\text{OH}$ in aqueous phase (7) will compete with the heterogeneous hydrodechlorination by atomic [H] on Pd surface (3) for TCE degradation. It has been noted that contaminant degradation by the Pd-containing electrolytic system can be enhanced by the addition of Fe(II) due to the increase in $\bullet\text{OH}$ accumulation.²⁶ With respect to TCE, both reduction and oxidation may happen depending on the relative rate of oxidation and reduction. As a consequence, it is important to reveal the pathways for TCE degradation in the Pd-containing electrolytic system in the presence of Fe(II).



In this study, the pathways of TCE degradation in an undivided Pd-containing electrolytic system are compared in the absence and presence of Fe(II) under weak acidic condition. Pd/Al₂O₃ is used as a catalyst for both atomic [H] and H₂O₂ generation. TCE degradation and $\bullet\text{OH}$ generation at different Fe(II) concentrations and pH values are investigated. The influence of Pd/Al₂O₃ dosage and groundwater chemistry on TCE degradation is also evaluated. The main objectives are: (1) to reveal the individual contribution of hydrodechlorination by atomic [H] and oxidation by $\bullet\text{OH}$ to TCE degradation in the absence and presence of low concentration of Fe(II); (2) to explore the relationship between TCE degradation and system parameters (Fe(II) concentration, pH and Pd/Al₂O₃ dosage), as well as $\bullet\text{OH}$ generation; and (3) if feasible, to propose a novel Pd-based electrochemical oxidation process for TCE remediation.

EXPERIMENTAL SECTION

Chemicals

TCE (99.5%) and cis-dichloroethylene (cis-DCE, 97%) were purchased from Sigma-Aldrich. Dichloroacetic acid (99%), glyoxylic acid (50% in water), glyconic acid (67% in water), sodium acetic trihydrate (100%), formaldehyde (37%) and H₂O₂ (30%) were purchased from Fisher Sci. Sodium oxalic (99.8%) and FeSO₄•7H₂O were purchased from J.T Baker. Other chemicals include gas standard (1% (v/v) methane, ethene, ethane, acetylene, CO₂ and CO in nitrogen, Supelco), dimethyl sulfoxide (DMSO, 99.9%, Acros), formic acid (88% in water, Acros Organics) and 2,4-dinitrophenylhydrazine (98.0%, Tokyo Chemical Industry Co., Ltd). Excess TCE was dissolved into 18.2 mΩ-cm high-purity water to form a TCE saturated solution (1.07 mg/mL at 20 °C), which was used as stock solution for preparing aqueous TCE solutions. Palladium on alumina powder (1% wt. Pd, Sigma-Aldrich) with average particle size of 6 μm was used as catalyst. Deionized water (18.0 mΩ-cm) obtained from a Millipore Milli-Q system was used in all the experiments. All chemicals used in this study were above analytical grade.

Degradation of TCE

An undivided acrylic electrolytic cell as shown in Figure S1 in the Supporting Information (SI) was used for TCE degradation at ambient temperature (25 ± 1 °C). A 150-mL syringe with plunger was connected to the cell, allowing gas expansion during electrolysis. The

quantitative collection of gas in the syringe was confirmed by the electrolysis of 10 mM Na₂SO₄ solution. Two pieces of mixed metal oxide (MMO, IrO₂/Ta₂O₅ coating on titanium mesh type, 3N International, USA) at 85 × 15 × 1.8 mm (length × width × thickness) were used as anode and cathode with 42 mm spacing in parallel position. For each test, 400 mL of 10 mM Na₂SO₄ solution was transferred into the cell, and 1 g/L Pd/Al₂O₃ and 13.6 mg/L Fe²⁺ concentrations were attained by addition of specific mass of Pd/Al₂O₃ powder and volume of Fe²⁺ stock solution. The dosage of Pd/Al₂O₃ and Fe²⁺ is selected according to experimental results. 10 mL of TCE saturated water was then added to produce an initial TCE concentration of 198 μM (26.1 mg/L). The reactor was sealed immediately and the solution was stirred for 10 min to allow equilibrium of TCE in the aqueous solution. Stirring at 600 rpm was maintained using a Teflon-coated magnetic stirring bar. A constant electric current of 100 mA (10 mA/cm²) was applied with a cell voltage of 7 V. The aqueous solution was sampled for analysis of TCE, *cis*-DCE, Cl⁻, organic acids, pH, oxidation reduction potential (ORP), Fe(II) and H₂O₂ concentrations. Gas samples were collected from specific experiment for headspace gas analysis.

For analyses of the degradation profile, the reactor was purged with N₂ for minutes to remove CO₂ before the addition of electrolyte. 1 mM Na₂SO₄ and 0.5 mM CaSO₄ were added to simulate groundwater chemistry. The initial concentration of TCE was doubled (396 μM) by adding 20 mL of TCE saturated water. All experiments were carried out in duplicate.

Chemical Analysis

TCE and *cis*-DCE were measured by a 1200 Infinity Series HPLC (Agilent) equipped with an 1260 DAD detector and an Agilent Poroshell 120 EC-C18 column (4.6 × 50 mm). The mobile phase was a mixture of acetonitrile and water (60:40, v/v) at 1 mL/min. The detection wavelength was 210 nm. Ethene and ethane in the headspace were detected by Model 310 GC (SRI, USA) with flame ionization detector and Haysep-T column. 100 μL of headspace gas was sampled and injected from an on-column port. The temperature program includes heating the column from 40 to 140 °C at a rate of 15 °C/min, holding the temperature at 140 °C for 1 min, and then cooling to 40 °C at a rate of 20 °C/min. The detection limits for TCE, *cis*-DCE and ethane were 0.1, 0.2 and 0.01 mg/L, respectively. CO₂ was absorbed in NaOH solution and measured for inorganic carbon by TOC analyzer. Chloride and carboxylic acidic intermediates were analyzed by a Dionex DX-5500 ion chromatograph. The •OH levels were determined with DMSO trapping and HPLC according to the literature.³⁰ The details for CO₂ and •OH analysis are provided in Sections S1 and S2 in the Supporting Information, respectively. Gas concentrations of TCE and *cis*-DCE along with the aqueous concentrations of ethane and CO₂ were calculated by Henry's law, and the sum of aqueous and gas concentrations was derived. H₂O₂ was measured at 405 nm by a spectrometer (Spectronic 20D+, Caley & Whitmore Corp.) after coloration with TiSO₄.³¹ The ferrous ion content was determined at 510 nm using the 1,10-o-phenanthroline analytical method.³²

Data Analysis

The commonly used pseudo first-order reaction kinetics model results in small correlation coefficients (R²) when modeling TCE transformation. A pseudo zeroth-order reaction kinetics (9) is more accurate and is used to fit TCE decay in time. The model is given by,

$$C_t = C_0 - k_0 t \quad (9)$$

where t is the reaction time (min), k_0 is the rate constant ($\mu\text{M}/\text{min}$), and c_0 and c_t are the concentrations (μM) at times of $t = 0$ and $t = t$, respectively. The production of Cl^- and $\bullet\text{OH}$ also followed pseudo zeroth-order reaction kinetics (10) given by,

$$C_t = k_0 t \quad (10)$$

Faradic current efficiency (CE, eq. 11) is used to evaluate the efficiency of electric energy consumption. It is assumed that the hydrodechlorination and oxidation of TCE require 8 and 6 electrons, respectively, for production of ethane and CO_2 . The current efficiency is given by,

$$\text{CE} = (C_t - C_0) \times 0.001 \times 0.41 \times zF / (I \bullet t) \quad (11)$$

where z is the number of electron transfer, F is Faradic constant (96485), I is current (A), 0.41 is the groundwater volume (L), and 0.001 denotes the transformation of concentration unit.

RESULTS AND DISCUSSION

Degradation of TCE in the Absence and Presence of Fe(II)

Figure 1 illustrates the degradation profiles of TCE in simulated groundwater in the absence and presence of Fe(II). Initial pH and Fe(II) concentration were set at 4 and 13.7 mg/L, respectively. Under identical conditions but without application of electricity, the addition of 1 g/L Pd/ Al_2O_3 did not cause any significant removal of TCE (Figure S2). Similarly, there was no significant removal by direct degradation on the MMO electrode. In presence of Pd/ Al_2O_3 and absence of Fe(II) (Figure 1a), TCE concentration decreased from 396 to 160 μM within 80 min with production of ethane and small fractions of *cis*-DCE and CO_2 . The high recoveries of carbon (>0.87) and Cl (>1.00) suggest that most degradation products are recovered. The production of ethane implies a dominant hydrodechlorination process, whereas the production of small fraction of CO_2 implies the minor contribution of oxidation to TCE degradation.

Presence of Fe(II) in the simulated groundwater greatly enhanced TCE degradation (Figure 1b) to 20.2 μM concentration after 80 min. The major products were CO_2 , followed by oxalic acid, ethane, acetic acid and *cis*-DCE, which all account for more than 80% of total carbon. This suggests that oxidation rather than hydrodechlorination is the main mechanism for TCE degradation in the presence of Fe(II). Other products reported in the literature for TCE oxidation such as dichloroacetic acid, glyoxylic acid, formic acid and ClO_3^- were not detected.^{5,33} The decay of TCE follows pseudo zeroth-order reaction kinetics, suggesting that the rates become increasingly limited by the availability of reactive species, i.e. $\bullet\text{OH}$, with increasing reactant concentrations.⁹ The rate constant for TCE decay increases from 3.1 $\mu\text{M}/\text{min}$ in the absence of Fe(II) to 4.9 $\mu\text{M}/\text{min}$ in the presence of Fe(II) (Table 1). This indicates that the oxidation pathway in the presence of Fe(II) is more effective than the hydrodechlorination pathway in the absence of Fe(II). In addition, the current efficiency for TCE degradation increased from around 15% to around 20% (Figure S3a) in the presence of Fe(II). Because relatively small concentrations of Fe(II) are used, the variation of cell voltage by the addition of Fe(II) is negligible. Therefore, improvement in energy utilization is achieved in the presence of Fe(II).

During the process, the aqueous pH in the absence and presence of Fe(II) decreased gradually from 4.00 to 3.10–3.20 (Figure S3b) due to production of HCl. However, the ORP in the absence of Fe(II) was significantly higher than that in the presence of Fe(II) (Figure

S3a), which is attributable to the role of Fe(II) in one case and accumulation of higher concentrations of H₂O₂ in the other case (Figure S3c). The production of H₂O₂ and its decomposition into •OH on Pd surface (6)^{22,23} may be the reason for generation of small fraction of CO₂ in the absence of Fe(II). However, the oxidation of TCE by H₂O₂ does not appear to be competitive in the absence of Fe(II) since hydrodechlorination dominated the degradation pathway. This is consistent with literature that reported unchanged degradation pathway in the presence of dissolved O₂,^{17,19} although the production of H₂O₂ was not considered. The presence of Fe(II) remarkably decreases the accumulated H₂O₂ concentrations because H₂O₂ can be decomposed by Fe(II) for generation of •OH by Fenton reaction (4). Although •OH has a much higher oxidation potential than H₂O₂ (standard potential: 2.80 versus 1.77 V/SHE), its lifespan is very short, only a few nanoseconds in water,³⁴ which was responsible for the lower ORP compared with that in the absence of Fe(II). Due to the lower regeneration rate of Fe(II) in Fenton chain reactions,^{26,34} dissolved Fe(II) concentration (Figure S3c) promptly decreased to below 1 mg/L regardless of the gradual decrease in solution pH. The zeroth-order kinetics imply that dissolved Fe(II) at such a low concentration was capable of generating a constant concentration of reactive species for TCE oxidation. This highlights the importance of Fe(II) in groundwater for the Pd-based degradation of TCE.

Although the shift in degradation pathway from hydrodechlorination to oxidation in Pd-based process has not been reported before, researchers in recent years reported the oxidizing ability of a reducing system, i.e. Fe-based process, in the presence of O₂. For example, the combination of zerovalent iron and dissolved O₂ has been recognized as an efficient oxidation technology,^{35,36} and contaminant oxidation instead of reduction was also identified as the dominant pathway in natural pyrite suspension in the presence of O₂.³³

Effect of Fe(II) Concentration on TCE Degradation and •OH Generation

Increasing Fe(II) concentration in the electrolyte improves the rate of TCE decay (Figure 2a). Zeroth-order decay rate constants increase from 2.0 to 4.6 μM/min when the initial Fe(II) concentration is increased from 0 to 27.3 mg/L (Table 1). Note that the lower rate for TCE decay in the absence of Fe(II) (compared to that in Figure 1a) is due to the use of different initial TCE concentrations and background electrolytes. The accumulated H₂O₂ concentrations decrease with the increase in Fe(II) concentrations (Figure 2b), which is in agreement with enhanced H₂O₂ decomposition. Figure 2c shows that the accumulated •OH concentrations also follow zeroth-order kinetics, and the rate increases with the increase in Fe(II) concentrations. The low concentrations of •OH measured in the absence of Fe(II) support the data showing production of CO₂ in the absence of Fe(II). The strong dependence of TCE decay and •OH generation on Fe(II) concentration is supported by their good correlation at initial Fe(II) concentrations of 0–13.7 mg/L (Figure 2d). In this electrolytic system, the concentrations of H₂O₂ produced were identical at any Fe(II) concentration. However, the actual concentration of Fe(II) became much lower than its initial concentration (Figure S3c), and the regeneration of Fe(II) from Fe(III) is much slower compared with the consumption.^{29,34} As the molar ratio of Fe(II) to H₂O₂ is less than the optimal values of about 1.0,^{29,37} the Fe(II)-dependent TCE decay and •OH generation occurs.

Moreover, a good correlation between TCE decay rate constants and •OH generation rate constants is obtained with a slope of 0.85 (the inset in Figure 2d), proving that •OH is the dominant reactive species for TCE degradation. The dependence of contaminant degradation and •OH generation is also noted by others,³⁵ but the correlation has never been reported.

Effect of pH and Pd/Al₂O₃ Dosage

TCE decay was negligible at pH 8.5 but increased dramatically with the drop of aqueous pH (Figure 3a). At high pH, the generation of H₂O₂ is limited,^{25,26} and most Fe²⁺ ions precipitate with OH⁻. With the drop of pH, both H₂O₂ generation and dissolved Fe(II) concentration increase contributing to accumulation of more •OH, as evident in Figure S4a. Likewise, zeroth-order rate constants for both TCE decay and •OH generation correlate well with initial pH values (Figure S4b). The pH-dependent contaminant degradation are the typical characteristics of Fenton-based oxidation,^{26,33–35} whereas the decrease in TCE hydrodechlorination is reported with drop in pH.²⁰ The correlation between TCE decay rate constants and •OH generation rate constants (the inset in Figure S4b) verify the predominant contribution of •OH to TCE degradation. The slope of the correlation reflects the sensitivity of TCE degradation to these parameters. The slope at different pHs is less than that obtained at different Fe(II) concentrations (0.67 versus 0.85), which indicates that pH plays a less important role than Fe(II) concentration for TCE degradation.

TCE degradation is also dependent on Pd/Al₂O₃ dose (Figure 3b). The plot of TCE decay rate constants versus Pd/Al₂O₃ dosage reveals good correlation at dosage higher than 0.2 g/L (Figure S5). The increase in Pd/Al₂O₃ dosage can facilitate the chemisorption of H₂ and the formation of atomic [H].³ Meanwhile, the chemisorption of O₂ is also enhanced.^{26,38} With the increase in Pd/Al₂O₃ dosage, more H₂O₂ are produced by the combination of the activated O₂ and [H]. As a result, more •OH is generated in the presence of Fe(II). Although the increase in Pd/Al₂O₃ dose may also enhance the hydrodechlorination process,³ its contribution is minimal as minute degradation was achieved at 1g/L Pd/Al₂O₃ in the absence of Fe(II) (Figure 2a).

Influence of Groundwater Chemistry on TCE Degradation

The results clearly suggest that oxidation by •OH in the presence of Fe(II) in an electrolytic system is more effective for TCE degradation compared with the hydrodechlorination by Pd•[H] in the absence of Fe(II). This provides a very powerful Pd-based oxidation rather than reduction for TCE remediation. To further assess the process, the influence of groundwater chemistry on TCE degradation was tested. Figure 4 shows that commonly present anions and cations in groundwater, including SO₄²⁻, Cl⁻, NO₃⁻, HCO₃⁻, Na⁺, K⁺, Ca²⁺ and Mg²⁺, at 10 mM do not cause any significant influence on the degradation. This is similar to reported results for chemisorption of H₂^{3,20} and contaminant oxidation by •OH.³⁹ The inhibitory effect of Cl⁻ on •OH-induced oxidation⁴⁰ occurs in the presence of high concentration (20 mM).

It is well established that sulfur at reduced state, i.e. SO₃²⁻ and S²⁻, dramatically deactivate Pd under anaerobic conditions,^{20,41} which is detrimental for application of Pd-catalytic hydrodechlorination in groundwater remediation. In this study, the presence of 1 mM SO₃²⁻ (112 mg/L) significantly enhances TCE degradation, and the presence of 31.3 μM S²⁻ (1 mg/L) results in a slight suppression (Figure 4a). In this electrolytic system, in situ generated H₂O₂, •OH and O₂ in aqueous solution as well as MMO anode may oxidize SO₃²⁻ and S²⁻ and prevent the deactivation of Pd.^{42,43} It is reported that the co-existence of MnO₄⁻ can oxidize reduced sulfur compounds preventing the poisoning of Pd for contaminant hydrodechlorination.⁴¹ The enhanced degradation in the presence of SO₃²⁻ is expected to be due to the presence of reactive oxygen species (O₂, H₂O₂, •OH, etc). It is also likely for the production of SO₃^{•-} and SO₄^{•-} anionic radicals by the oxidation of sulfite in this Pd-containing electrolytic system,⁴⁴ thereby enhancing TCE oxidation. The underlying mechanism for the enhancement will be explored in our future work.

Kinetics Analysis

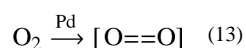
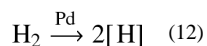
•OH is identified as the reactive species responsible for TCE degradation in the presence of Fe(II). Under testing conditions, a linear increase in cumulative •OH concentration is measured (Figures 2 and S4) indicating a constant rate of •OH generation. Due to the extremely short lifespan of •OH in water (a few nanoseconds),³⁴ a very low steady-state concentration of •OH in solution can be inferred. TCE oxidation by •OH is a homogeneous quick reaction ($(3.3\text{--}4.3) \times 10^9 \text{ mol}^{-1} \text{ s}^{-1}$),⁴⁵ and diffusion process is fast when solution is being stirred. As a consequence, the generated •OH is immediately consumed by TCE, leading to an apparent zeroth-order degradation kinetics. When •OH oxidation is not the dominant pathway, i.e. in presence of very low concentration of Fe(II), low dosage of Pd/Al₂O₃ or at high pH, a deviation from zeroth-order kinetics is observed, as indicated by the decrease in correlation coefficient (R^2 in Table 1).

Since •OH is mainly generated by the quick combination of Fe²⁺ and H₂O₂ ($k = 63 \text{ M}^{-1} \text{ s}^{-1}$),³⁴ both Fe(II) and H₂O₂ concentrations affect TCE degradation. When initial Fe(II) concentration is lower than 13.7 mg/L or solution pH is higher than 4, the availability of free Fe(II) determines TCE degradation (Figure 2). When Fe(II) concentration is higher than 13.7 mg/L, the availability of H₂O₂ affects TCE degradation. When Pd/Al₂O₃ is sufficient (> 1 g/L), dissolution of H₂ and O₂, the source reactants for H₂O₂ production, as well as their chemisorption on Pd surface influence the degradation. Because chemisorption of O₂ on Pd is much more difficult compared with H₂, it is assumed to be the rate-limiting step for H₂O₂ synthesis from equimolar H₂ and O₂.^{38,46} In the electrolytic system, the molar ratio of H₂ and O₂ produced at the cathode (2) and anode (1), respectively, is 2:1, whereas the aqueous solubility of H₂ (0.81 mM) is higher than half of that of O₂ (1.25 mM). Therefore, chemisorption of O₂ on Pd surface is also a rate-limiting step for TCE degradation.

Degradation Mechanism in the Absence and Presence of Fe(II)

The mechanisms of TCE degradation in the absence and presence of Fe(II) are summarized in Scheme 1. H₂ produced at the cathode (2) dissolves in the electrolyte and diffuses onto the surface of Pd catalyst, where it undergoes chemisorption and decomposition to two atomic [H] (12). H₂ adsorption on Pd surface is strong at room temperature resulting in an almost equivalent ratio of [H] to surface Pd atom.⁴⁷ During the electrolysis the [H] concentration on Pd surface can be considered constant because H₂ is continuously produced at cathode. In the absence of Fe(II), TCE undergoes hydrodechlorination on Pd surface by [H] to cis-DCE, ethene, and finally hydrogenation to ethane.

Meanwhile, O₂ produced at the anode (1) also dissolves in the electrolyte and diffuses onto the surface of Pd catalyst. The chemisorption of O₂ molecule on Pd surface elongates the O=O double bond (13).³⁸ The chemisorbed O₂ competes with TCE for [H] and produce H₂O₂ (5). Pd can catalyze the decomposition of H₂O₂ to •OH,^{25,26} which leads to slight oxidation in the absence of Fe(II). The pathway for TCE hydrodechlorination by [H] in the presence of dissolved O₂ is similar to those reported in the literature.^{17,19} However, the slight contribution of oxidation induced by •OH was never reported and is noted for the first time in this study.



On the other hand when Fe(II) is present in the solution, the generation of •OH in aqueous solution is dramatically enhanced through the combination of Fe(II) and H₂O₂ (8). Further, as the generated •OH is present in aqueous solution, mass transfer poses a much less pronounced effect for TCE oxidation compared with hydrodechlorination on Pd surface. Both lead to a more competitive oxidation than hydrodechlorination for TCE degradation. As a consequence, the dominant pathway for TCE degradation shifts from heterogeneous hydrodechlorination on Pd surface in the absence of Fe(II) to homogeneous oxidation in aqueous solution in the presence of Fe(II). The oxidation of TCE by •OH leads to the production of organic acids, and finally CO₂.

Implications

This study reveals the production of H₂O₂ in the presence of O₂ using Pd-based catalyst and H₂. The generation of low concentrations of •OH slightly contributes to TCE oxidation under weak acidic conditions. In particular, when Fe(II) is present, H₂O₂ efficiently decomposes to •OH resulting in a shift in dominant pathway from heterogeneous hydrodechlorination to homogeneous oxidation. This shift is most pronounced at high Fe(II) concentrations and low pH values. These findings may contribute to understanding the nature for chlorinated solvent degradation by Pd-catalytic hydrodechlorination in the presence of O₂, especially when Fe(II) at a level of ppm is present.

In the Pd-containing electrolytic system, oxidation of TCE in the presence Fe(II) is proved to be significantly more efficient than hydrodechlorination in the absence Fe(II) under weak acidic conditions. Moreover, complete dechlorination is achieved with production of nontoxic organic acids and CO₂. A comparison with Fenton remediation by H₂O₂ addition suggests that the proposed process is more advantageous in both TCE degradation and Fe(II) regeneration (Figure S6). As a result, a novel Pd-based oxidation process using electro-generated H₂ and O₂ is proposed, although further evaluation and assessment is required prior to any field evaluation. Figure S7 depicts a conceptual model for remediation, wherein the desired low pH condition is achieved automatically by a modified three-electrode system.²⁶ When contaminated groundwater flows through the anode and Cathode 1 installed in a single well, it will be saturated with electro-generated O₂ and H₂. Because a specific (designed) fraction of the current is shared by Cathode 2, H⁺ ions produced at the anode is more than OH⁻ ions produced at Cathode 1, and an in-situ drop of pH to 3–4 can be reached by the design.²⁶ Under these conditions, H₂O₂ is produced on the Pd catalyst packed. Fe(II) intrinsically contained in groundwater or added externally catalyzes the generation of •OH from H₂O₂. Note that the automatically developed low pH condition can also increase the dissolved Fe(II) concentration, thereby enhancing contaminant oxidation. Contaminants in groundwater are then oxidized or even mineralized. The second cathode installed will neutralize the acidic effluent. Our current work includes conducting column experiments to evaluate the performance of this model.

Supplementary Material

Refer to Web version on PubMed Central for supplementary material.

Acknowledgments

This work was supported by the National Institute of Environmental Health Sciences (NIEHS, Grant No. P42ES017198), the Natural Science Foundation of China (NSFC, No.40801114, 41172220), and the Fundamental Research Funds for the Central Universities, China University of Geosciences (Wuhan) (No. CUGL110608). The content is solely the responsibility of the authors and does not necessarily represent the official views of the NIEHS or the National Institutes of Health. We appreciate valuable suggestions from three anonymous reviewers.

References

1. Rabideau AJ, Blayden JM, Ganguly C. Field performance of air sparging system for removing TCE from groundwater. *Environ Sci Technol.* 1999; 33:157–162.
2. Tsitonaki A, Petri B, Crimi M, Mosbaek H, Siegrist RL, Bjerg PL. In situ chemical oxidation of contaminated soil and groundwater using persulfate: A review. *Crit Rev Environ Sci Technol.* 2010; 40:55–91.
3. HF, Zhao D. Hydrodechlorination of trichloroethene using stabilized Fe-Pd nanoparticles: Reaction mechanism and effects of stabilizers, catalysts and reaction conditions. *Appl Catal B Environ.* 2008; 84:533–540.
4. Lee W, Batchelor B. Abiotic reductive dechlorination of chlorinated ethylenes by iron-bearing phyllosilicates. *Chemosphere.* 2004; 56:999–1009. [PubMed: 15268967]
5. Carter KE, Farrell J. Electrochemical oxidation of trichloroethylene using boron-doped diamond film electrodes. *Environ Sci Technol.* 2009; 43:8350–8354. [PubMed: 19924968]
6. Petersen MA, Sale TC, Reardon KF. Electrolytic trichloroethene degradation using mixed metal oxide coated titanium mesh electrodes. *Chemosphere.* 2007; 67:1573–1581. [PubMed: 17234239]
7. Mccarty PL, Goltz MN, Hopkins GD, Dolan ME, Allan JP, Kawakami BT, Carrothers TJ. Full-scale evaluation of in situ cometabolic degradation of trichloroethylene in groundwater through toluene injection. *Environ Sci Technol.* 1998; 32:88–100.
8. Al-Abed SR, Fang YX. Use of granular graphite for electrolytic dechlorination of trichloroethylene. *Environ Eng Sci.* 2007; 24:842–851.
9. Mishra D, Liao Z, Farrell J. Understanding reductive dechlorination of trichloroethene on boron-doped diamond film electrodes. *Environ Sci Technol.* 2008; 42:9344–9349. [PubMed: 19174914]
10. Reddy, KR.; Cameselle, C. *Electrochemical remediation technologies for polluted soils, sediments and groundwater.* John Wiley & Sons, Inc; 2009.
11. Mao XH, Ciblak A, Amiri M, Alshawabkeh AN. Redox control for electrochemical dechlorination of trichloroethylene in bicarbonate aqueous media. *Environ Sci Technol.* 2011; 45:6517–6523. [PubMed: 21671641]
12. Lohner ST, Becker D, Mangold KM, Tiehm A. Sequential reductive and oxidative biodegradation of chloroethenes stimulated in a coupled bio-electro-process. *Environ Sci Technol.* 2011; 45:6491–6497. [PubMed: 21678913]
13. Chen G, Betterton EA, Arnold RG, Ela WP. Electrolytic reduction of trichloroethylene and chloroform at a Pt- or Pd-coated ceramic cathode. *J Appl Electrochem.* 2003; 33 (2):161–169.
14. Franz JA, Williams RJ, Flora JRV, Meadows ME, Irwin WG. Electrolytic oxygen generation for subsurface delivery: Effect of precipitation at the cathode and an assessment of side reactions. *Water Res.* 2002:2243–2254. [PubMed: 12108717]
15. Lohner ST, Tiehm A. Application of electrolysis to stimulate microbial reductive PCE dechlorination and oxidative VC biodegradation. *Environ Sci Technol.* 2009; 43:7098–7104. [PubMed: 19806748]
16. Weathers LJ, Parkin GF, Alvarez PJJ. Utilization of cathodic hydrogen as an electron donor for chloroform metabolism by a mixed methanogenic culture. *Environ Sci Technol.* 1997; 31:880–885.
17. McNab WW JR, Ruiz R. Palladium-catalyzed reductive dehalogenation of dissolved chlorinated aliphatics using electrolytically-generated hydrogen. *Chemosphere.* 1998; 37:925–936.
18. Gent DB, Wani AH, Davis JL, Alshawabkeh A. Electrolytic redox and electrochemical generated alkanline hydrolysis of hexahydro-1,3,5-trinitro-1,3,5 triazine (RDX) in sand columns. *Environ Sci Technol.* 2009; 43:6301–6307. [PubMed: 19746729]
19. Lowry GV, Reinhard M. Pd-catalyzed TCE dechlorination in water: Effects of $[H_2](aq)$ and H_2 -utilizing competitive solutes on the TCE dechlorination rate and product distribution. *Environ Sci Technol.* 2001; 35:696–702. [PubMed: 11349280]
20. Lowry GV, Reinhard M. Pd-catalyzed TCE dechlorination in groundwater: Solute effects, biological control, and oxidative catalyst regeneration. *Environ Sci Technol.* 2000; 34:3217–3223.

21. Nutt MO, Hughes JB, Wong MS. Designing Pd-on-Au bimetallic nanoparticle catalysts for trichloroethene hydrodechlorination. *Environ Sci Technol.* 2005; 39:1346–1353. [PubMed: 15787376]
22. Hildebrand H, Mackenzie K, Kopinke FD. Highly active Pd-on-magnetite nanocatalysts for aqueous phase hydrodechlorination reactions. *Environ Sci Technol.* 2009; 43:3254–3259. [PubMed: 19534143]
23. Schueth C, Kummer NA, Weidenthaler C, Schad H. Field application of a tailored catalyst for hydrodechlorinating chlorinated hydrocarbon contaminants in groundwater. *Appl Catal B.* 2004; 52:197–203.
24. Edwards JK, Solsona B, Ntainjua NE, Carley AF, Herzing AA, Kiely CJ, Hutchings GJ. Switching off hydrogen peroxide hydrogenation in the direct synthesis process. *Science.* 2009; 323:1037–1041. [PubMed: 19229032]
25. Choudhary VR, Samanta C, Jana P. Decomposition and/or hydrogenation of hydrogen peroxide over Pd/Al₂O₃ catalyst in aqueous medium: Factors affecting the rate of H₂O₂ destruction in the presence of hydrogen. *Appl Catal A.* 2007; 332:70–78.
26. Yuan SH, Fan Y, Zhang YC, Tong M, Liao P. Pd-catalytic in situ generation of H₂O₂ from H₂ and O₂ produced by water electrolysis for the efficient electro-Fenton degradation of rhodamine B. *Environ Sci Technol.* 2011; 45:8514–8520. [PubMed: 21866953]
27. Ravikumar JX, Gurol MD. Chemical oxidation of chlorinated organics by hydrogen peroxide in the presence of sand. *Environ Sci Technol.* 1994; 28:394–400. [PubMed: 22165872]
28. Iron & manganese in groundwater, Water Stewardship Information Series. B.C.'s Ground Water Protection Regulation; 2007. [http://www.env.gov.bc.ca/wsd/plan_protect_sustain/groundwater/library/ground_fact_sheets/pdfs/fe_mg\(020715\)_fin2.pdf](http://www.env.gov.bc.ca/wsd/plan_protect_sustain/groundwater/library/ground_fact_sheets/pdfs/fe_mg(020715)_fin2.pdf)
29. Neyens E, Baeyens J. A review of classic Fenton's peroxidation as an advanced oxidation technique. *J Hazard Mater.* 2003; B98:33–55. [PubMed: 12628776]
30. Tai C, Peng JF, Liu JF, Jiang GB, Zou H. Determination of hydroxyl radicals in advanced oxidation processes with dimethyl sulfoxide trapping and liquid chromatography. *Anal Chim Acta.* 2004; 527:73–80.
31. Eisenberg G. Colorimetric determination of hydrogen peroxide. *Ind Eng Chem Anal Ed.* 1943; 15:327–328.
32. Komadel P, Stucki JW. Quantitative assay of minerals for iron(II) and iron(III) using 1,10-phenanthroline. III. A rapid photochemical method. *Clays Clay Miner.* 1988; 36:379–381.
33. Pham HT, Suto K, Inoue C. Trichloroethylene transformation in aerobic pyrite suspension: Pathways and kinetic modeling. *Environ Sci Technol.* 2009; 43:6744–6749. [PubMed: 19764244]
34. Brillas E, Sirés I, Oturan A. Electro-Fenton process and related electrochemical technologies based on Fenton's reaction chemistry. *Chem Rev.* 2009; 109:6570–6631. [PubMed: 19839579]
35. Joo SH, Feitz AJ, Sedlak DL, Waite TD. Quantification of the oxidizing capacity of nanoparticulate zero-valent iron. *Environ Sci Technol.* 2005; 39:1263–1268. [PubMed: 15787365]
36. Stieber M, Putschew A, Jekel M. Treatment of pharmaceuticals and diagnostic agents using zero-valent iron – Kinetic studies and assessment of transformation products assay. *Environ Sci Technol.* 2011; 45:4944–4950. [PubMed: 21539306]
37. Arnold SM, Hickey WJ, Harris RF. Degradation of atrazine by Fenton's reagent: Condition optimization and product quantification. *Environ Sci Technol.* 1995; 29:2083–2089. [PubMed: 22191359]
38. Staykov A, Kamachi T, Ishihara T, Yoshizawa K. Theoretical study of the direct synthesis of H₂O₂ on Pd and Pd/Au surfaces. *J Phys Chem C.* 2008; 112:19501–19505.
39. Chaplin BP, Schrader G, Farrell J. Electrochemical destruction of N-nitrosodimethylamine in reverse osmosis concentrates using boron-doped diamond film electrodes. *Environ Sci Technol.* 2010; 44:4264–4269. [PubMed: 20441141]
40. Kiwi J, Lopez A, Nadochenko V. Mechanism and kinetics of the OH-radical intervention during Fenton oxidation in the presence of a significant amount of radical scavenger (Cl⁻). *Environ Sci Technol.* 2000; 34:2162–2168.

41. Angeles-Wedler D, Mackenzie K, Kopinke FD. Permanganate oxidation of sulfur compounds to prevent poisoning of Pd catalysts in water treatment processes. *Environ Sci Technol.* 2008; 42:5734–5739. [PubMed: 18754501]
42. Hoffmann MR. Kinetics and mechanism of oxidation of hydrogen sulfide by hydrogen peroxide in acidic solution. *Environ Sci Technol.* 1977; 11:61–66.
43. Pikaar I, Rozendal RA, Yuan Z, Keller J, Rabaey K. Electrochemical sulfide oxidation from domestic wastewater using mixed metal-coated titanium electrodes. *Water Res.* 2011; 45:5381–5388. [PubMed: 21885081]
44. Neta P, Huie RE. Free-radical chemistry of sulfite. *Environ Health Persp.* 1985; 64:209–217.
45. Chen G, Hoag GE, Chedda P, Nadim F, Woody BA, Dobbs GM. The mechanism and applicability of in situ oxidation of trichloroethylene with Fenton's reagent. *J Hazard Mater.* 2001; B87:171–186. [PubMed: 11566408]
46. Samanta C. Direct synthesis of hydrogen peroxide from hydrogen and oxygen: An overview of recent developments in the process. *Appl Catal A.* 2008:133–149.
47. Chen H, Xu Z, Wan H, Zheng J, Yin D, Zheng S. Aqueous bromate reduction by catalytic hydrogenation over Pd/Al₂O₃ catalysts. *Appl Catal B Environ.* 2010; 96:307–313.

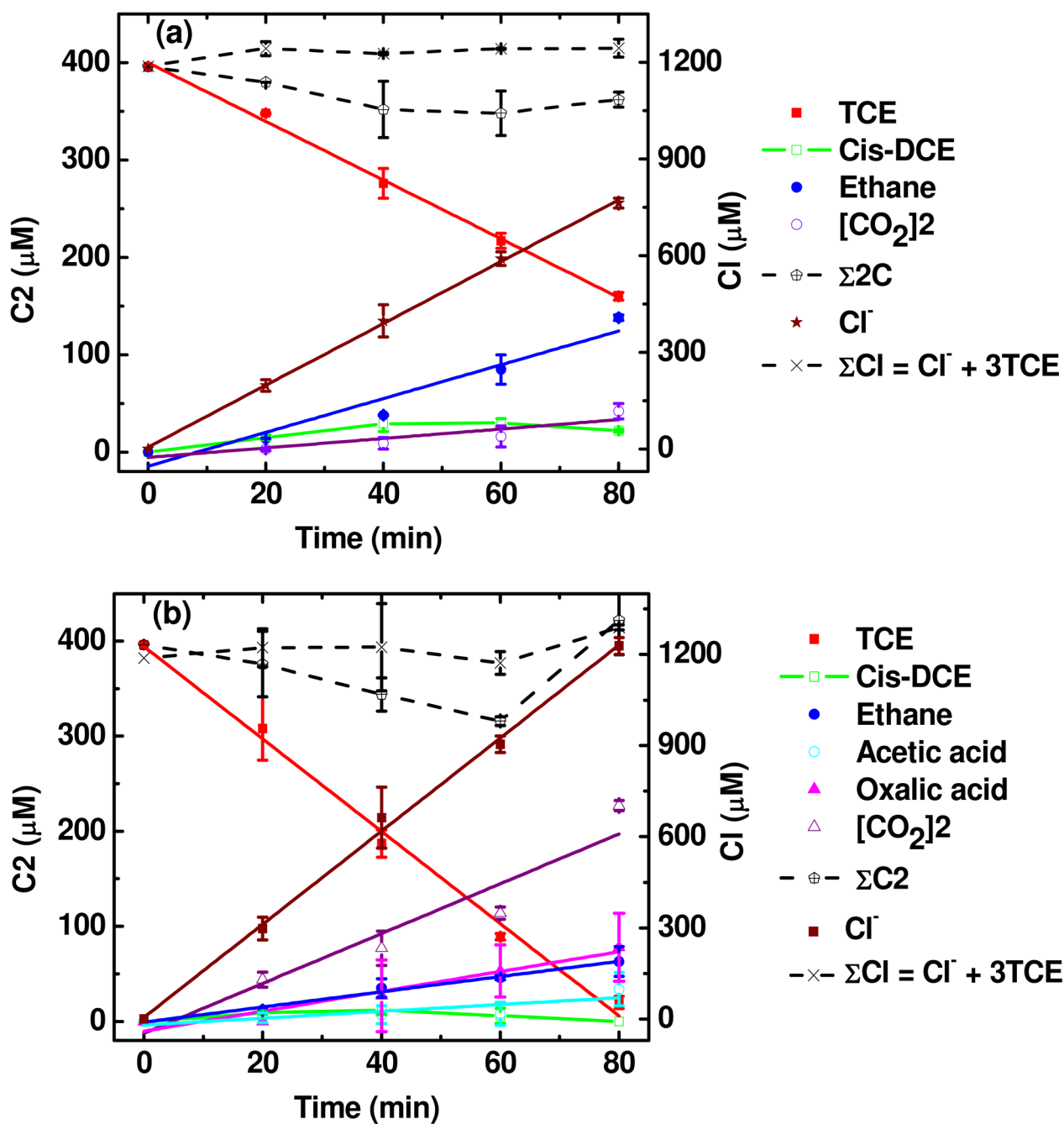


Figure 1.

Degradation profiles of TCE (a) without Fe(II) (b) with Fe(II). [CO₂]₂ stands for the half concentration of CO₂ accumulated. Lines denote the linear fit of the data points in the same color. The degradation conditions are based on 396 μM initial TCE concentration, initial pH 4.0, 1 g/L Pd/Al₂O₃, 1 mM Na₂SO₄ and 0.5 mM CaSO₄, and 13.6 mg/L Fe(II) concentration when present.

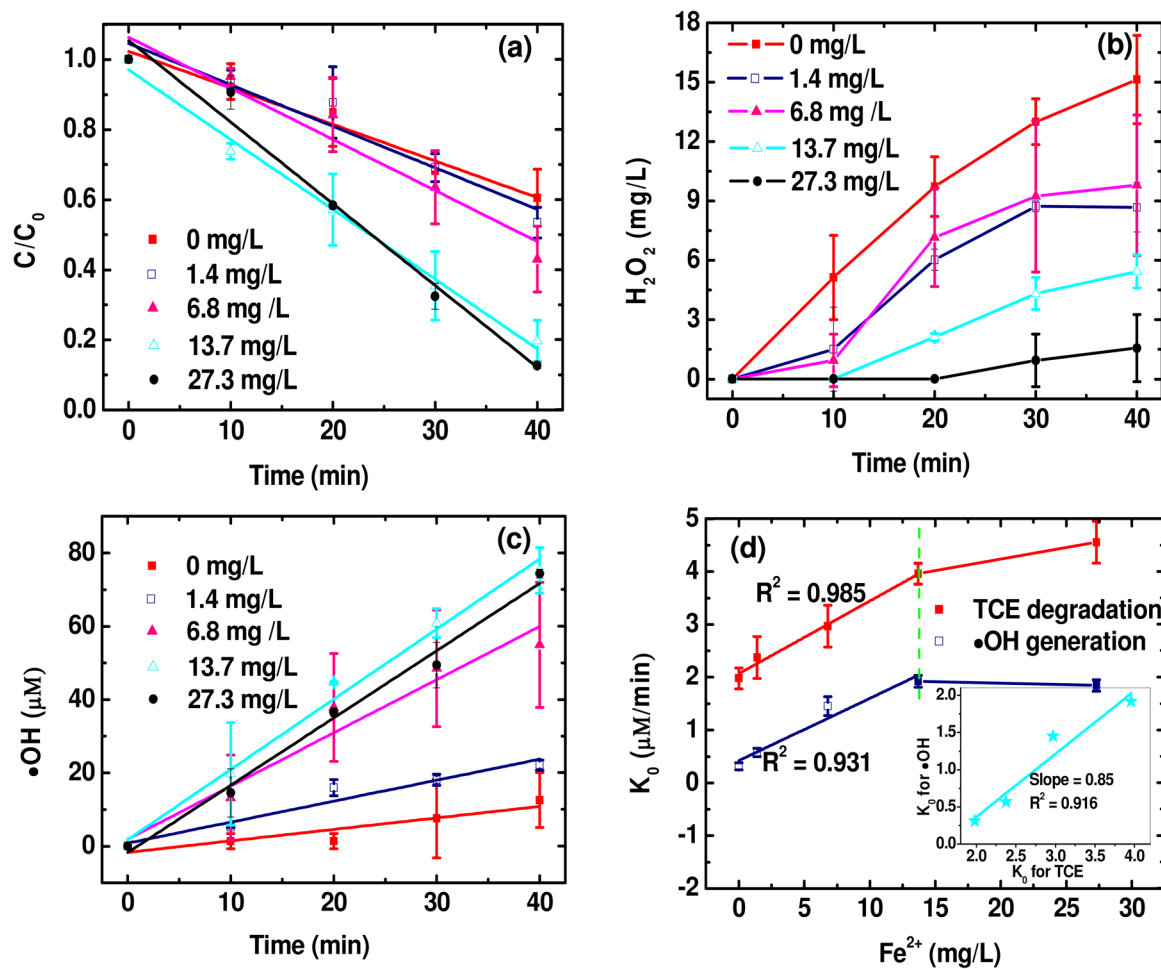


Figure 2.

Effect of initial Fe(II) concentration on (a) TCE decay, (b) H₂O₂ production and (c) •OH generation; and (d) the plots of Fe(II) concentrations versus K₀ for TCE decay and •OH generation. The inset in (d) illustrates linear regression of the zeroth-order rate constants for •OH generation and TCE decay. Lines denote the linear fit of the data points in the same color. The reaction conditions are based on 198 μM initial TCE concentration, pH 4, 1 g/L Pd/Al₂O₃ and 10 mM Na₂SO₄.

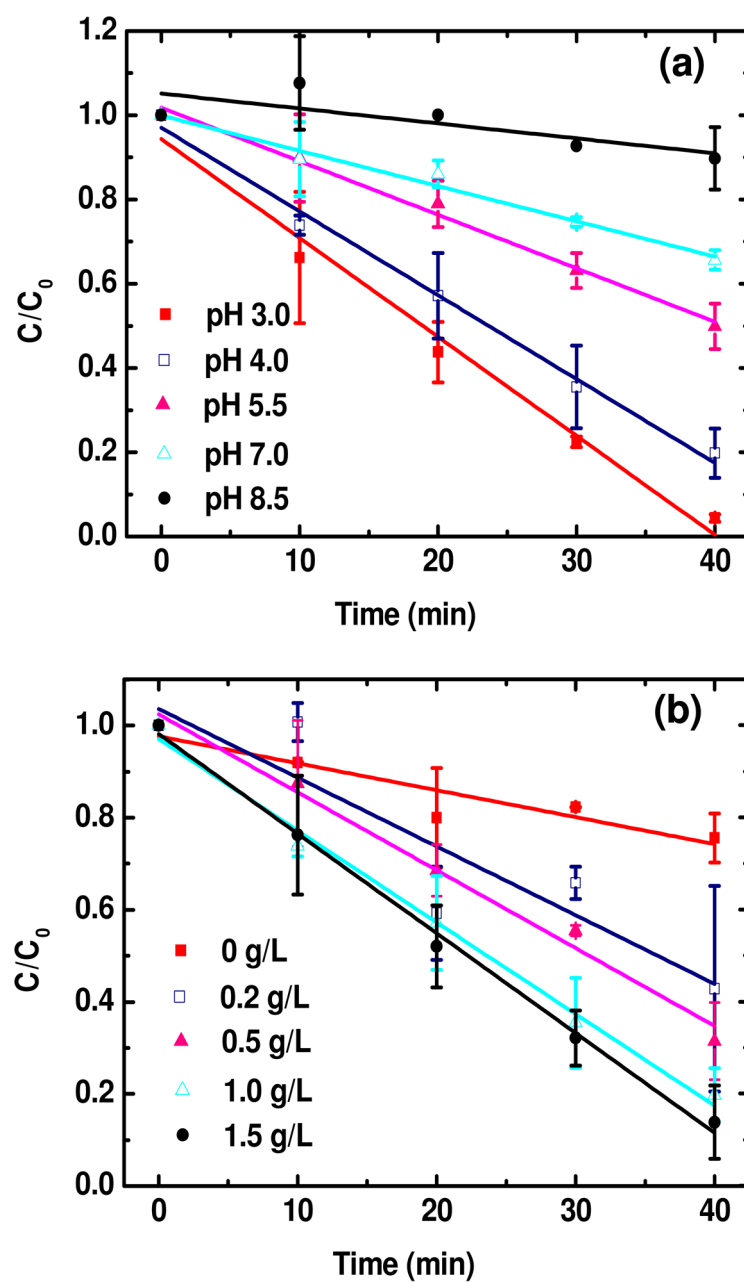


Figure 3. Effect of (a) pH and (b) Pd/Al₂O₃ dosage on TCE degradation. Lines denote the linear fit of the data points in the same color. Otherwise stated, the reaction conditions are based on 198 μ M initial TCE concentration, 13.7 mg/L Fe(II), pH 4, 1 g/L Pd/Al₂O₃ and 10 mM Na₂SO₄.

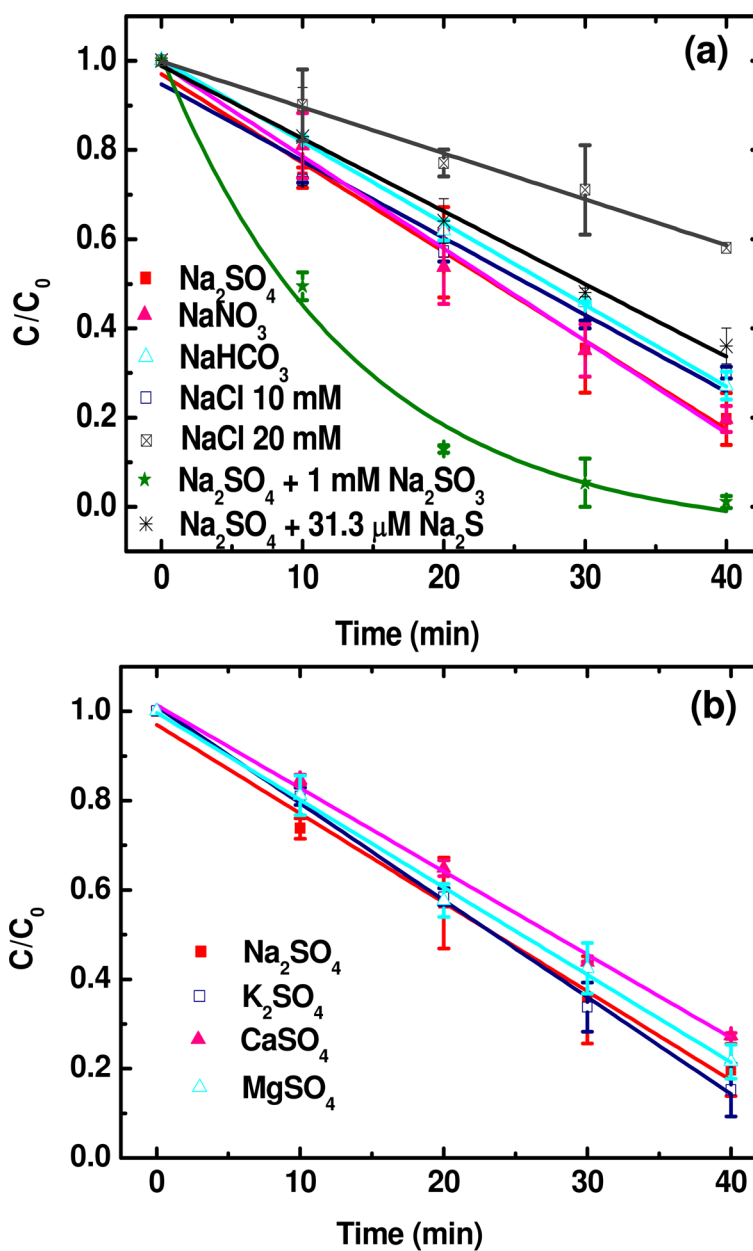
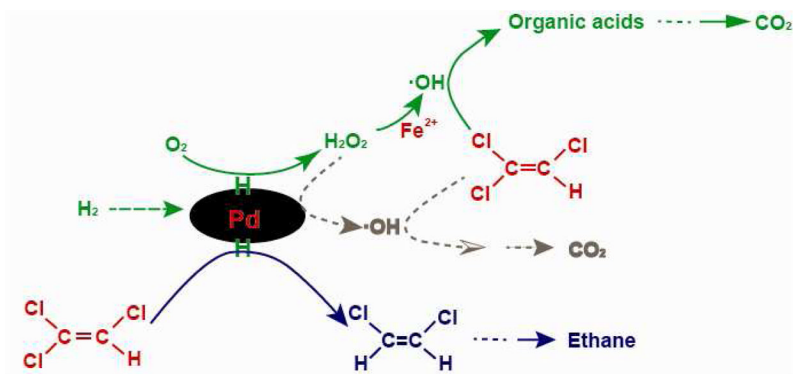


Figure 4. Effect of (a) anionic and (b) cationic ions in solution on TCE degradation. Lines denote the linear fit of the data points in the same color. The reaction conditions are based on 198 μM initial TCE concentration, 13.7 mg/L Fe(II), pH 4 and 1 g/L Pd/Al₂O₃, and 10 mM electrolyte unless specified.



Scheme 1.
Mechanism for TCE degradation in the absence and presence of Fe(II)

Table 1

Results Summarized for TCE Degradation

no.	Variation parameters ^a	pH		Residue TCE (μM)	k ₀ ^b μM/min	R ² for k ₀
		initial	final			
1 ^c	396 μM TCE + 13.6 mg/L Fe(II)	4.00	3.10 ± 0.01	20.2 ± 6.6	4.9 ± 0.3	0.990
2 ^c	396 μM TCE + 0 mg/L Fe(II)	4.00	3.17 ± 0.03	160.4 ± 4.2	3.1 ± 0.1	0.996
3	0 mg/L Fe(II)	4.00	3.94 ± 0.03	122.8 ± 21.8	2.0 ± 0.2	0.965
4	1.4 mg/L Fe(II)	4.00	3.70 ± 0.07	105.7 ± 8.6	2.4 ± 0.4	0.924
5	6.8 mg/L Fe(II)	4.00	3.53 ± 0.07	85.1 ± 18.5	3.0 ± 0.4	0.925
6	13.7 mg/L Fe(II)	4.00	3.29 ± 0.02	39.0 ± 11.6	4.0 ± 0.2	0.990
7	27.3 mg/L Fe(II)	4.00	3.18 ± 0.03	24.9 ± 1.6	4.6 ± 0.4	0.973
8	pH 3.0	3.00	2.91 ± 0.01	8.7 ± 1.7	4.6 ± 0.4	0.980
9	pH 4.0	4.00	3.27 ± 0.04	39.0 ± 11.6	4.0 ± 0.2	0.990
10	pH 5.5	5.50	3.95 ± 0.18	98.5 ± 10.7	2.6 ± 0.2	0.990
11	pH 7.0	7.00	5.80 ± 0.46	129.9 ± 4.6	1.6 ± 0.2	0.976
12	pH 8.5	8.50	6.51 ± 1.61	177.7 ± 14.7	0.8 ± 0.4	0.519
13	0 g/L Pd/Al ₂ O ₃	4.00	3.45 ± 0.04	149.8 ± 10.5	1.2 ± 0.2	0.837
14	0.2 g/L Pd/Al ₂ O ₃	4.00	3.29 ± 0.02	84.8 ± 44.2	3.0 ± 0.8	0.789
15	0.5 g/L Pd/Al ₂ O ₃	4.00	3.27 ± 0.04	62.1 ± 16.5	3.4 ± 0.2	0.984
16	1.0 g/L Pd/Al ₂ O ₃	4.00	3.29 ± 0.02	39.0 ± 11.6	4.0 ± 0.2	0.990
17	1.5 g/L Pd/Al ₂ O ₃	4.00	3.35 ± 0.01	27.4 ± 15.7	4.4 ± 0.2	0.995
18	10 mM Na ₂ SO ₄	4.00	3.29 ± 0.02	39.0 ± 11.6	4.0 ± 0.2	0.990
19	10 mM NaCl	4.00	3.23 ± 0.04	59.4 ± 2.6	3.4 ± 0.4	0.966
20	20 mM NaCl	4.00	3.50 ± 0.02	83.2 ± 0.0	2.0 ± 0.1	0.988
21	10 mM NaNO ₃	4.00	3.44 ± 0.06	38.8 ± 5.7	4.2 ± 0.2	0.988
22	10 mM NaHCO ₃	4.00	3.68 ± 0.01	53.6 ± 6.2	3.6 ± 0.2	0.998
23	10 mM K ₂ SO ₄	4.00	3.63 ± 0.17	30.2 ± 11.7	4.4 ± 0.2	0.997
24	10 mM CaSO ₄	4.00	3.58 ± 0.08	54.1 ± 1.2	3.8 ± 0.2	0.997
25	10 mM MgSO ₄	4.00	2.98 ± 0.07	42.5 ± 7.5	4.0 ± 0.2	0.996
26	10 mM Na ₂ SO ₄ + 31.3 μM Na ₂ S	4.00	3.28 ± 0.01	71.5 ± 6.9	3.2 ± 0.1	0.992

no.	Variation parameters ^a	pH		Residue TCE (μM)	k_0 ^b $\mu\text{M}/\text{min}$	R^2 for k_0
		initial	final			
27	10 mM Na_2SO_4 + 1 mM Na_2SO_3	4.00	3.35 ± 0.06	1.9 ± 2.7	$0.11 \pm 0.01 \text{ min}^{-1} d$	0.975

^a Otherwise stated, the reaction conditions are based on 198 μM TCE, 13.7 mg/L Fe(II), pH 4, 1 g/L Pd/Al₂O₃, 10 mM Na_2SO_4 and 40 min degradation.

^b k_0 is the zeroth-order decay rate constant.

^c The background electrolyte consists of 1 mM Na_2SO_4 and 0.5 mM CaSO_4 , and the degradation time is 80 min.

^d A pseudo first-order rate constant ($\ln C_0/C_t = K_1 t + b$, where K_1 is the rate constant) is provided.